Joint Centre for Mesoscale Meteorology, Reading, UK

Layer-wise attribution of vertical motion and the influence of potential-vorticity anomalies on synoptic development

JCMM Internal Report No 134

NWP Scientific Paper No 67

May 2002

M A G Dixon

A J Thorpe

K A Browning

Met Office Joint Centre for Mesoscale Meteorology Department of Meteorology
University of Reading PO Box 243 Reading RG6 6BB United Kingdom
Tel: +44 (0)118 931 8425 Fax: +44 (0)118 931 8791
www.metoffice.com

Designed and produced by the Met Office © Crown copyright 2002 02/0392
Met Office and the Met Office logo are registered trademarks

Layer-wise attribution of vertical motion and the influence of potential-vorticity anomalies on synoptic development

By M. A. G. Dixon* †, A. J. Thorpe, K. A. Browning

University of Reading, UK

SUMMARY

A methodology is presented for attributing vertical motion to potential vorticity (PV) in an unambiguous manner using the quasi-geostrophic (QG) omega equation. The methodology is then used to determine the contribution individual PV anomalies make to the synoptic development. It is shown how the total vertical motion may be decomposed into self-generating and interaction terms. The former correspond to vertical motion that arises from one PV region alone, whilst each of the interaction terms represent vertical motion due to the interaction of two different regions of PV. The new methodology is applied to a number of FASTEX cyclones in order to determine the dynamical role of individual PV regions in cyclogenesis. For purposes of comparison, cyclones were chosen to be representative of the types (A,B, and C) of an extended Petterssen-Smebye scheme devised by Deveson, Browning and Hewson. In terms of the new PV methodology, the Type A and B cyclones exhibit only subtle differences, with the upper-level layer of PV playing a larger role in the case of the Type B cyclone. A much larger difference is apparent between the Type A and B cyclones on the one hand, and the Type C cyclone on the other: in the Type C cyclone, the upper-level PV self-generating term plays an important role, whereas in the Type A and B cases the influence of the upper-level PV is largely restricted to the interaction terms. In all of the cases, the forcing attributable to the interaction between the low-level PV and boundary thermal gradient was found to be large. Hence, from the viewpoint of instantaneous forcing, we conclude that the low-level PV is always important. However, from a viewpoint which considers the influence of one PV region on another, it appears that in some cyclones (Type C) the upper-level PV plays a much larger role in the overall control of the forcing.

1. INTRODUCTION

This paper sets out a methodology by which vertical motion may be attributed to regions of quasi-geostrophic (QG) potential vorticity (PV) in an unambiguous manner. In short, this is achieved by making explicit that part of the vertical motion which is attributable to the interaction of separate PV regions. The methodology establishes an important diagnostic link, hitherto absent from 'QGPV-thinking', between PV and dynamical development. We demonstrate the usefulness of this link by considering the specific case of mid-latitude cyclone development.

It has long been recognised that PV-thinking provides a powerful way of understanding dynamical development (Hoskins et al, 1985). Apart from the inherent interest of determining the dynamical significance of a particular region of PV, there are at least two advantages of doing so from the viewpoint of forecasting. As PV, in the absence of diabatic processes, is materially conserved then it is relatively easy to predict the advection of a given PV region. Thus, if at a given instant one could determine which PV region is most dynamically significant, observations could be targeted so that the PV region is accurately assimilated into an analysis at a later time. By way of contrast, if one were to view the forcing of vertical motion in terms of sources that are not materially conserved, then the procedure of targeting would become more difficult.

Determining which regions of PV are dynamically significant may also be helpful in terms of model improvement. PV provides a link between diabatic processes and their ensuing effects on the dynamics. That is, diabatic processes lead to local changes in the PV distribution which, in turn, may lead to dynamical development. Given this property,

* Current affiliation: Met Office

† Corresponding author: Joint Centre for Mesoscale Meteorology (JCMM), Department of Meteorology, University of Reading, PO Box 243, Reading, Berkshire, RG6 6BB, UK.

it is an attractive idea to validate model parameterizations of diabatic processes in terms of the PV anomalies created.

The attribution of vertical motion *per se* is a well-known technique of analysing dynamical development. The procedure normally adopted involves the use of an omega-equation, wherein the total vertical motion is partitioned into components attributable to particular 'sources'. A number of sources have been considered, including the 'traditional' choices of thermal advection (TA) and differential vorticity advection (VA). This choice of source underpins the cyclone classification scheme of Petterssen & Smebye (1971) (PS). The frame-independent choice of $\nabla.\mathbf{Q}$ (Hoskins et al., 1978 and Clough et al., 1996), has recently been used by Deveson et al. (2001), (DBH), to develop a modified version of the PS scheme. According to this scheme, cyclones are classified partly in terms of the relative importance of the upper- and lower-level distributions of $\nabla.\mathbf{Q}$. It is important to note, however, that neither of these schemes address the question of cyclone development in terms of PV.

Two versions of so-called 'PV-surgery' have been adopted in an attempt to attribute dynamic effects to specific regions of PV. On the one hand, some studies (eg Griffiths et al. (2000), Thorpe (1997) Davis & Emanuel (1991)) assess the dynamical significance of a PV region in a *diagnostic* sense by either calculating the difference in vertical motion between an unaltered atmospheric state and another where the PV region has been removed, or by assessing the effect on development of the horizontal wind fields attributable to a region of PV. The alternative, *prognostic* approach involves measuring the impact on a time-evolving model of removing the PV region from the initial model state (see, for example, Ahmadi-Givi & Craig, 2001, Swarbrick, 2001). Both approaches share a central ambiguity: the dynamical impact which is nominally attributed to a particular PV region depends upon the rest of the total PV distribution.

The methodology presented in this paper addresses the ambiguity from a diagnostic perspective by partitioning the total QG vertical motion which is nominally attributable to a given region of PV into several components. Each component is attributable either to that PV region alone (the so-called 'self-generating' part), or to the 'interaction' between the region and other 'elements' in the domain, where these elements are either PV regions or are identified with boundary conditions. Whilst the resulting conceptual picture is complicated by the existence of the 'interaction' terms, it is argued that this is nevertheless the correct manner in which to proceed with the diagnostic PV attribution of vertical motion. The usefulness of the methodology in determining the dynamical significance of PV regions will be illustrated via case studies of mid-latitude cyclones. For simplicity, we have adopted a 'layer-wise' approach, wherein the total PV distribution is partitioned into three components, *viz.* an upper and a lower slab, and an infinitesimal layer at the surface. Such a partitioning also facilitates a comparison with the DBH classification scheme, and in order to highlight the difference between attributing dynamical development to PV on the one hand, and $\nabla.\mathbf{Q}$ on the other hand, we apply the new methodology to cyclones representative of the three classes (Types A, B and C) of the DBH scheme.

2. The Omega Equation

The QG omega equation can be written as:

$$\mathrm{L}(\omega) = S \tag{1}$$

where the operator

$$L \equiv \nabla_p^2 + \frac{f_o^2}{\sigma}\frac{\partial^2}{\partial p^2}. \tag{2}$$

where p is the pressure; f_o is the Coriolis parameter; σ is the static stability; and the subscript p denotes that the 2-D Laplacian is applied on a constant pressure surface.

Clough *et al.* (1996), expanding on the ideas of Thorpe and Bishop (1995), used an electrostatics analogy as an illuminating way of physically interpreting Eq. (1), wherein the source term, S, is analogous to a distribution of charge and the vertical motion, ω, is akin to the electric field associated with that charge. Thus, the vertical motion field is said to be *attributable* to the source distribution. This paper is concerned with 'layer-wise' attribution, i.e. the process by which the total ω is partitioned into components, each of which is attributable to a layer of S. We next consider the various mathematical formulations of S which were referred to in the introductory section. The physical interpretation of each, along with some of the ways in which the resulting conceptual pictures have been applied in the literature will be discussed.

(*a*) *Traditional formulation*

The 'traditional' form of the source term (see, for example, Hoskins *et al.*, 1978) is given by:

$$S = f_o\frac{\partial}{\partial p}\left[(\mathbf{v}-\mathbf{c}).\nabla_p\xi\right] + R\nabla^2\left[(\mathbf{v}-\mathbf{c}).\nabla_p\theta\right] \tag{3}$$

where $\mathbf{c}$ is the velocity of the reference frame with respect to which the velocity fields, $\mathbf{v}$, are expressed; ξ is the vorticity; θ is the potential temperature and R is the universal gas constant. The two terms are referred to as (differential) vorticity advection (VA) and thermal advection (TA), respectively.

Petterssen and Smebye (1971) set out a classification scheme (PS) which defines two types of cyclone. Roughly speaking *, 'Type A' cyclones are those which are predominately forced by TA in the lower part of the atmosphere, whereas 'Type B' cyclones are forced mainly by VA in the upper levels. However, from Eq. (3) it is clear that both VA and TA are dependent on the choice of $\mathbf{c}$. Hence, such a classification scheme is ambiguous since the determination of whether TA or VA forcing dominates in a particular cyclone requires a reference frame to be specified. Such ambiguity has long been appreciated, and the 'Q-vector' formulation of the omega equation introduced by Hoskins *et al.* (1978) is a method of avoiding such difficulties.

(*b*) *Q-vector formulation*

In this formulation the source is given by:

$$S = -2.\nabla.\mathbf{Q} \tag{4}$$

The longitudinal (λ) and latitudinal (ϕ) components of the Q-vector, $\mathbf{Q} = [Q_1, Q_2]$, are given by:

* The PS scheme does in fact use further criteria to distinguish the two types of cyclone, such as the relative distance between upper-level troughs and surface lows; more to the point, it makes reference the time-dependency of such quantities. Nevertheless, the distinction described in the text here is the main determinant of whether a cyclone is of type A or B.

$$Q_1 = -\frac{Rp^{R/c_p-1}}{p_o^{R/c_p}}\frac{1}{a\cos\phi}\frac{\partial \mathbf{v}}{\partial\lambda}.\nabla\theta$$
$$Q_2 = -\frac{Rp^{R/c_p-1}}{p_o^{R/c_p}}\frac{1}{a}\frac{\partial \mathbf{v}}{\partial\phi}.\nabla\theta \qquad (5)$$

where c_p is the specific heat, p_o is the reference pressure and a is the radius of the Earth.

Note that $\mathbf{Q} = \mathbf{Q}(\mathbf{v}, T)$ and, since $\mathbf{v}$ and T both depend upon the streamfunction, that $\mathbf{Q}$ is a quadratic function of the streamfunction. This will be of relevance in later sections. It is evident that Eq. (4) is frame-invariant and hence the attribution of vertical motion in terms of Q-vectors is unambiguous.

The usefulness of this formulation is demonstrated in Deveson *et al.* (2001) who apply a modified version of the PS scheme, where the $\nabla.\mathbf{Q}$ distribution is partitioned into upper- and lower-level slabs. Cyclones are then classified according to the relative forcing of the upper and lower slabs, without the need to specify a reference frame. Whilst this procedure is valid, it is a common misconception that such a partitioning of the forcing of vertical motion, is either identical, or a close enough approximation to, a partitioning into upper- and lower-level slabs of PV. Hence, for example, Mansfield (1996) assumes that since the upper-level distribution of $\nabla.\mathbf{Q}$ contributes less to the vertical motion close to a cyclone centre than does the low-level slab of $\nabla.\mathbf{Q}$, then the upper-level PV distribution must also be relatively insignificant. Such reasoning is also evident in Davies and Bishop (1994), where PS Type 'B' cyclones are identified as those whose forcing is dominated by upper-level PV anomalies (rather than by VA). Central to the message of this paper, however, is that PV regions can lead to $\nabla.\mathbf{Q}$ sources which are (i) located remotely from the PV; and (ii) are heavily dependent on other sources of PV. This will be discussed more fully below; it suffices here to point out two implications of this in the context of layer-wise attribution. The first is that it is not possible to assess the contribution to the total vertical motion which is attributable to the upper-level PV distribution by simply calculating the vertical motion due to the upper-level $\nabla.\mathbf{Q}$ distribution alone: owing to the non-local nature of the $\mathbf{Q}$ field attributable to PV, the upper-level PV will lead to $\nabla.\mathbf{Q}$ located in the 'lower' atmosphere and similarly, low-level PV will lead to $\nabla.\mathbf{Q}$ sources in the upper atmosphere. Secondly, the upper-level and lower-level PV sources, along with the non-local effects of the temperature at the boundaries, interact to form $\nabla.\mathbf{Q}$ sources throughout both the upper and lower levels.

(c) *HMR formulation*

In the formulation of the omega equation presented by Hoskins, McIntyre and Robertson (1985), (HMR), the vertical motion is expressed as a sum of three parts, one of which is attributable to the differential advection of PV (see Eq. (6) below). Even given this explicit reference to PV, however, this method still does not provide a means of explicitly determining the vertical motion attributable to a given PV anomaly. The reason for this is that the other two remaining components of the vertical motion are also (albeit implicit) functions of the PV field. Nevertheless, this formulation is illuminating as regards to the physical origin of vertical motion, and will prove to be useful in interpreting the new methodology presented in this paper.

The total omega is given by the following sum:

$$\omega = \omega_{PVA} + \omega_{BTA} + \omega_{IU} \qquad (6)$$

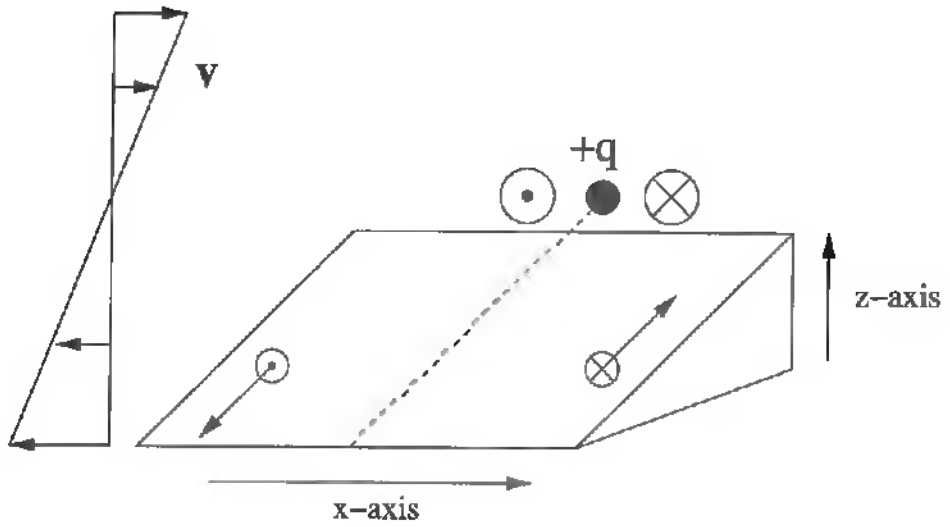

Figure 1. A schematic representation of how vertical motion arises from the interaction between (i) the horizontal wind fields (indicated by the circles) attributable to the point source of PV; and (ii) the sloping potential temperature surfaces associated with the sheared flow of the basic state

The first two terms represent contributions due to PV-advection (PVA) and boundary temperature advection (BTA) respectively. These vertical velocities are determined via the solution of Poission equations. It is possible to eliminate the BTA term by viewing the boundary temperature distribution as an infinitesimally thin sheet of PV located just above the surface, and including it in the source term of the PVA equation (Bretherton, 1966). This incorporation will be assumed from henceforth so that out of these first two terms, only the PVA need be considered.

The PVA term is given by:

$$L(\omega_{PVA}) = f_o \frac{\partial}{\partial p} [(\mathbf{v} - \mathbf{c}).\nabla_p q] \tag{7}$$

where q is the PV and $\omega_{PVA} = 0$ on the boundaries.

The remaining contribution, the isentropic up-glide term (IU), is evaluated *locally* and is given by:

$$\omega_{IU} = -(\mathbf{v} - \mathbf{c}).\nabla_p \theta' / (d\theta_{ref}/dp) \tag{8}$$

where θ denotes deviations from the reference state potential temperature, θ_{ref}.

Consider a point PV anomaly placed in an Eady-type basic state of constant shear (Figure 1). In the rest frame of the anomaly, ω_{IU} represents the total vertical motion. Splitting the horizontal velocity and temperature into contributions from the point anomaly (denoted by the subscript PV) and the basic state (labelled b) leads to:

$$\omega_{IU} \propto -(\mathbf{v}_{PV} - \mathbf{c}).\nabla_p \theta_b - (\mathbf{v}_b - \mathbf{c}).\nabla_p \theta_{PV} \tag{9}$$

Note that the 'self-generating' terms which arise from the velocity and potential-temperature fields attributable to either one of the sources alone are identically zero, and the total vertical motion is given (in Eq. (9)) by the sum of the two remaining 'interaction' terms. The first of these corresponds to the horizontal velocity field attributable to the PV anomaly causing parcels to 'ride up' the tilted isentropes of the basic state (Figure

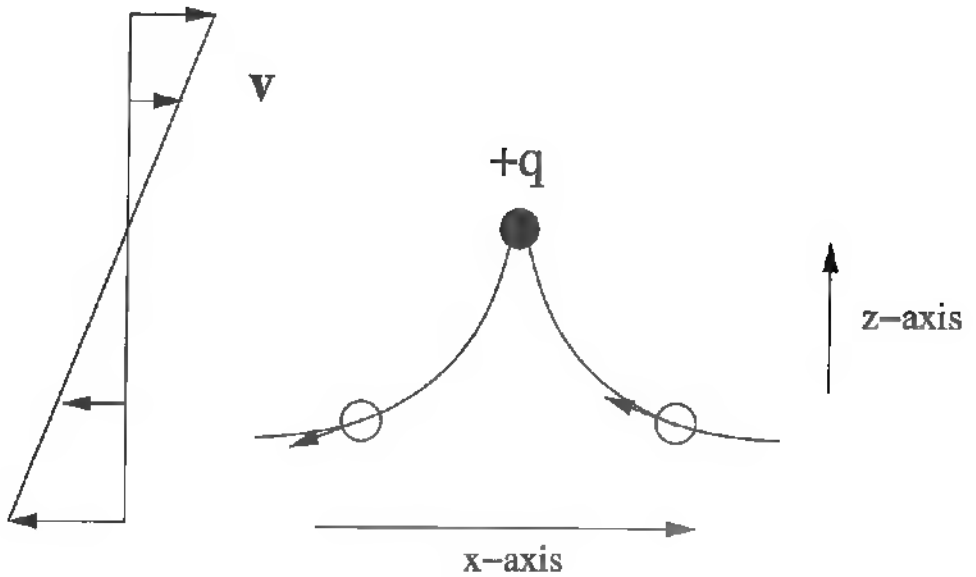

Figure 2. As in Figure 1, but here the vertical motion arises from the interaction between the basic state wind and the potential-temperature field attributable to the PV anomaly

1). The second (and smaller) term is due to the basic state zonal velocity causing parcels to ride up the bent isentropes associated with the PV anomaly (Figure 2).

Now consider the vertical motion at one particular location. If we switch to the rest frame of a parcel at this position, the IU term goes to zero and the PVA velocity equals the total vertical motion. Thus, the remote differential advection of PV acts like the local IU mechanism described above. At every other location, however, the resulting vertical motion is given by a combination of PVA and IU velocities, and the direct link between vertical motion and PV is lost. Of course, since this simplified system only consists of a basic state and one anomaly of PV, we know that the total vertical motion is always due to the interaction between these two elements. However, more realistic systems will consist of distributions of such point anomalies. It might be thought that in such cases, it would be possible to determine the vertical motion attributable to a subset of these anomalies by 'tuning' c to the velocity of their rest frame so that the IU term by itself describes their contribution. However, the IU term will be due in some part to the PV sources moving at velocities other than c.

3. Explicit Layer-wise PV Attribution of vertical Motion

In this section it is shown how vertical motion may be unambiguously attributed to layers of PV. The process we adopt consists of first splitting the wind and potential-temperature fields, of which the source term (Eq. (4)) is a function, into parts which are attributable to each part of the PV distribution. These fields are, in turn, derived from the perturbation streamfunctions.

A perturbation streamfunction, ψ', attributable to a perturbation source of PV, q' can be obtained by inverting the QGPV equation:

$$\nabla_h \psi' + \frac{\partial}{\partial p}\left(\frac{f_o}{\sigma}\frac{\partial \psi'}{\partial p}\right) = q' \tag{10}$$

We could partition the q' and hence the streamfunction, into as many components as we wish, but for this study we choose just three components. The first two components are related directly to the interior PV distribution. Investigations of the forcing of vertical motion (and, indeed, of forcing *per se*) are often posed in terms of the relative importance of the upper and lower levels of the atmosphere. For this reason we have chosen to partition the total PV distribution into upper and lower level slabs, leading to associated streamfunctions defined as follows:

1. ψ'_U - the streamfunction which is attributable to all of the PV located in the 'upper-levels', q_U (defined to be the layer ranging from 600mb to 150mb inclusively),
2. ψ'_L - the streamfunction which is attributable to all of the PV located in the 'lower-levels', q_L (i.e. 950mb to 650mb inclusive),

where we have assumed that the PV and all other fields are defined on a grid of 50mb vertical resolution.

The 'layer-wise' inversion process involves arbitrary choice of boundary conditions. The procedure usually adopted is to set the vertical derivative of the streamfunction (or equivalently, the potential temperature) equal to zero on the horizontal boundaries, so that the temperature on the boundaries may be considered as a separate distribution whose evolution is coupled to that of the interior PV via horizontal winds alone. In what follows, we set the temperature at the lower and upper surfaces (i.e. 1000mb and 100mb) attributable to the interior PV (be it 'upper' or 'lower') to zero. On the other boundaries, $\psi'_U = \psi'_L = 0$.

This leaves only the third contribution to the total streamfunction, which we shall refer to as the 'boundary' component:

$$\psi'_B = \psi'_{total} - (\psi'_U + \psi'_L) \tag{11}$$

where ψ'_{total} can be obtained, via geostrophy, from the total geopotential. This boundary component can be further divided into three sub-components. The first part is due to the temperature distributions on the upper and lower boundaries, which (as mentioned above) can be viewed as infinitesimal sheets of PV. The two other components arise from PV regions located outside the domain in which Eq.(10) was calculated, and from the lateral boundary conditions (as described in Bishop and Thorpe (1994), setting $\psi' = 0$ on the boundaries can be viewed as leading to the creation of image charges of PV). We assume that, as long as the streamfunction is evaluated close to the lower boundary and far from the lateral boundaries, ψ'_B (and indeed any vertical motion which is attributable to it) will be dominated by the effects of the lower boundary temperature distribution. This approximation is valid at each position of the cyclones considered in the next section.

Now, because of Eq. (1) and as $\mathbf{Q} = \mathbf{Q}(\mathbf{v}, \theta)$, we can write symbolically that $\omega = \omega(\mathbf{v}, \theta)$. As $\mathbf{Q}$ depends on the products of $\mathbf{v}$ and θ, then if we partition $\mathbf{v}$ and θ into three components each, the result is that there are nine individual terms for ω.

If the wind and potential-temperature fields in Eq. (4), which are related to the horizontal and vertical derivatives of the streamfunction, are partitioned into the three components corresponding to the streamfunctions defined above, then Eq. (2) leads to the following key expression for the total vertical motion:

$$\begin{aligned} \omega &= \omega(\mathbf{v}_U, \theta_U) + \omega(\mathbf{v}_L, \theta_L) + \omega(\mathbf{v}_B, \theta_B) \\ &+ \omega(\mathbf{v}_U, \theta_L) + \omega(\mathbf{v}_L, \theta_U) \end{aligned}$$

$$
\begin{aligned}
&+ \quad \omega(\mathbf{v}_U, \theta_B) + \omega(\mathbf{v}_B, \theta_U) \\
&+ \quad \omega(\mathbf{v}_L, \theta_B) + \omega(\mathbf{v}_B, \theta_L)
\end{aligned}
\tag{12}
$$

The three velocities on the first line of Eq. (12) represent the *self-generating* terms and are each due to the interaction of the potential-temperature and wind fields attributable to one element alone. Thus, for example, the first term corresponds to the vertical motion associated with the upper-level PV distribution alone. The final three lines of Eq. (12) contain the *interaction* terms which arise from the temperature field attributable to one layer interacting with the winds of another layer and vice versa.* Since both the potential temperature and horizontal velocity fields are derived from streamfunctions, arguably it would be more meaningful to decompose the vertical motion in terms of the streamfunctions alone. This would lead to a total of six components opposed to the nine in Eq. (12). If we write

$$
\begin{aligned}
\omega(\mathbf{v}_U, \theta_U) &= \omega(U, U) \\
\omega(\mathbf{v}_L, \theta_L) &= \omega(L, L) \\
\omega(\mathbf{v}_B, \theta_B) &= \omega(B, B)
\end{aligned}
\tag{13}
$$

and also,

$$
\begin{aligned}
\omega(\mathbf{v}_L, \theta_U) + \omega(\mathbf{v}_U, \theta_L) &= \omega(U, L) \\
\omega(\mathbf{v}_U, \theta_B) + \omega(\mathbf{v}_B, \theta_U) &= \omega(U, B) \\
\omega(\mathbf{v}_L, \theta_B) + \omega(\mathbf{v}_B, \theta_L) &= \omega(L, B)
\end{aligned}
\tag{14}
$$

we can write the sum of the six terms as:

$$
\begin{aligned}
\omega &= \omega(U, U) + \omega(L, L) + \omega(B, B) \\
&+ \omega(U, L) + \omega(U, B) + \omega(L, B)
\end{aligned}
\tag{15}
$$

In Section 4 we will consider the decomposition given by Eq. (15); however, we will also interpret the forcing in terms of Eq. (14) both for the sake of completeness and because this decomposition provides a more direct physical understanding (analogous to the example given in section 2(iii), above).

4. Application: attribution of cyclone forcing

In this section, we consider an important application of the layer-wise attribution of vertical motion: the determination of the role PV layers play in the development of extra-tropical cyclones.

(*a*) *Method*

* Note that if we partitioned the streamfunction in the way described in the last section and then calculated the *sum* of PVA and IU terms or the *sum* of TA and VA terms due to each of the nine combinations of temperature and velocity fields, then we would necessarily arrive at the same decomposition stated in Eq. (12).

In what follows, we interpret the rate of 'development' as the rate of change in vorticity following a cyclone. We define the cyclone location as the position of the local minimum of geopotential on the 900mb level. The material derivative of geostrophic vorticity, ζ_g evaluated using the velocity, **c**, of the cyclone centre is given by:

$$D_c(f+\zeta_g) = (\mathbf{c}-\mathbf{u}).\nabla(f+\xi) + f\frac{\partial\omega}{\partial p} \tag{16}$$

The advection term can be assumed to be small in the cyclone's frame of reference, and hence Eq. (16) may be approximated as:

$$D_c(f+\zeta_g)|_{900mb} \approx \frac{f}{\Delta}(\omega|_{800mb} - \omega|_{surface}) = \frac{f}{\Delta}.\omega|_{800mb} \tag{17}$$

where the omega at 1000mb has been set to zero and Δ is equal to 200mb. We make the further assumption that the development of the cyclone as a whole may be assessed by evaluating Eq. (17) at the grid point corresponding to the local maximum vertical motion on the 800mb surface. Attributing the cyclone forcing to layers of PV amounts to evaluating Eq. (17) at this point using each of the components given in Eq. (12) or Eq. (15). Henceforth, when we refer to any of the component terms of these two equations we will be implicitly referring to their values at this point. We have applied the methodology described to a number of cyclones, but before presenting the results, we first discuss the physical interpretation of the methodology in more detail and highlight some features which we expect to be shared by *all* cyclones.

(*b*) *Physical Interpretation*

(i) *The PV distribution in a mid-latitude cyclone*

Figure 3 shows a schematic cross-section through a mid-latitude cyclone. The upper-level QGPV distribution may be viewed as consisting of two components: the large-scale PV transition associated with the sloping tropopause, and a smaller scale PV 'anomaly' identified as a local 'fold' in the tropopause. In the lower levels, the background PV is small and homogeneous, with local PV anomalies (ultimately due to diabatic effects) dominating. Also evident in Figure 3 is the lower-boundary potential temperature distribution. It is important to note a distinction between the case depicted in Figure 3 and that of the idealised example of section 2(iii). In the idealised case, the basic-state wind and potential-temperature fields are, in a sense, artificially imposed as they are not directly attributable to PV within the domain. In contrast, the large-scale fields in Figure 3 are attributable partly to PV within the domain. In fact, they are mainly a consequence of the PV associated with the sloping tropopause and the surface temperature gradient, with the anomalies making a smaller contribution.

(ii) *The self-generating terms*

Consider the self-generating terms of Eq. (12). Imagine a PV anomaly placed within a barotropic basic state. If the anomaly is symmetrical (in the QG-scaled coordinate $\sqrt{x^2+y^2+\frac{\sigma^2 p^2}{f_o^2}}$) then it is straightforward to show that no vertical motion will be generated. Thus, for example, the point PV anomaly considered in section 2(iii) has no self-generated vertical motion associated with it. The same would be true of the low-level PV region in Figure 3 if the low-level anomaly were perfectly symmetrical. As this is not true in general, $\omega(L, L)$ will be finite and, hence, contribute to the cyclone's development.

The nature of the upper-level PV self-generated motion, $\omega(U, U)$, is complicated by the presence of the PV associated with the sloping tropopause. Part of $\omega(U, U)$ will be

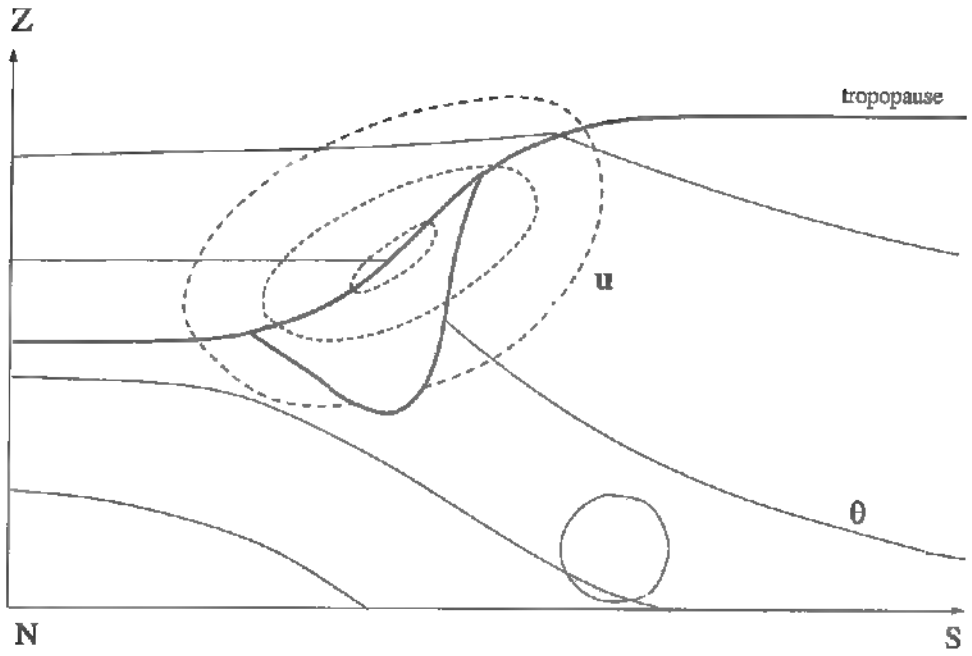

Figure 3. A schematic cross-section through a mid latitude cyclone. A few contours of horizontal wind (dashed lines) and potential temperature (full lines) are shown. The tropopause marks the large scale PV transition and the upper- and lower-level PV anomalies are indicated by the shaded areas.

due to the interaction between the fields attributable to the large-scale PV transition and those fields attributable to the local PV anomaly. In addition, if the PV anomaly displays asymmetry, then part of $\omega(U, U)$ will be due to the anomaly alone. If there are no upper-level PV anomalies, on the other hand, then $\omega(U, U)$ will be zero.

The self generating contribution to cyclone development from the lower boundary term, $\omega(B, B)$, is likely to be small. This can be understood by interpreting our methodology in terms of the Eady problem (see, for example, Davies & Bishop, 1994). In that problem, edge waves constrained to the upper and lower boundaries grow in amplitude owing to their interaction. This interaction is mediated via the basic state of uniform baroclinic shear. Note that, just as in section 2 (iii), the basic state of the Eady problem is artificially imposed. Nevertheless the PV distribution on the lower boundary may be thought of as an edge wave, and as such, the wind and potential temperature fields attributable to this distribution will act in such a way as to propagate the surface temperature anomaly without any concomitant growth. This edge-wave-like distribution will have no associated self-generated vertical motion; it is only via the interaction with the 'basic-state' that growth and vertical motion occur.

(iii) *Interaction Terms*

For any of the interaction terms to be finite, the morphology of the two relevant regions of PV must differ. To see this, imagine a symmetrical anomaly, such as the point anomaly of section 2 (iii), in a barotropic background flow. The introduction of a second anomaly, identical in shape at the same position as the first, would not lead to any vertical motion. It is only by shifting the relative positions of the anomalies and/or altering their shapes, that any 'interaction' vertical motion can be generated. One would expect there to be much scope for differences between the morphologies of the three PV regions in a

mid-latitude cyclone, implying that the interaction terms may play an important role in cyclone forcing.

Of all the interaction terms, it is likely that $\omega(L, B)$ will play the most significant role in most cyclones. This is simply because of the relative proximity of a low-level PV anomaly and of the boundary PV distribution to the location of the cyclone. The wind and potential temperature fields attributable to both of these PV regions will be large in the vicinity of the cyclone and, as long as these fields differ significantly in terms of their morphology, they will lead to large $\nabla.\mathbf{Q}$ and hence large vertical motion close to the cyclone. Owing to the greater distance between the upper-level PV and the cyclone, we may expect $\omega(U, B)$ and $\omega(U, L)$ to be less significant than $\omega(L, B)$ in general.

Of the two components of $\omega(L, B)$, it is likely that $\omega(v_L, \theta_B)$ will be larger than $\omega(v_B, \theta_L)$. This difference can be understood by referring to the idealised example presented in section 2(c). Since the sign of θ_{PV} changes with height, the $\nabla.\mathbf{Q}$ distribution that is attributable to θ_{PV} and $\mathbf{v}_b$ forms a vertical dipole. The resulting vertical motion is relatively smaller than that associated with θ_b and $\mathbf{v}_{PV}$, owing to destructive interference between the two parts of the aforementioned the dipole. We can apply such reasoning to the real case of $\omega(L, B)$ since the low-level PV tends to be relatively localised and the fields associated with the boundary PV are similar to that of the basic state in the idealised example. However, the reasoning may be less relevant in the case of $\omega(U, B)$ and its component elements because, although the upper-level PV distribution may contain anomalies, it is also composed of the transition associated with the sloping tropopause (which bears a strong resemblance to the boundary PV distribution).

(c) *FASTEX Case Studies*

The methodology described above has has been applied to a total of four cyclones which occured during the FASTEX campaign (see Joly *et al.*, 1999). So as to highlight the differences between our new approach and that of the method by which cyclone forcing is attributed to parts of the $\nabla.\mathbf{Q}$ distribution, these cyclones have been picked according to the classification scheme of DBH, which assessed the forcing of each cyclone in terms of the vertical motion at 700mb. * In addition to the Type A and B cyclones proposed in the original PS scheme, DBH identified 'Type C' cyclones, which are more strongly upper-level forced than those of 'Type B'. The four cyclones considered below, labelled by their FASTEX 'Intensive Observation Period' (IOP) numbers, were chosen according to the following criteria. IOP9 and IOP14 were the strongest low-level forced 'Type A' cyclones; IOP11A was a middle-of the-range 'Type B' cyclone; and IOP18 was the strongest upper-level forced 'Type C' cyclone.

The data used are analyses and T+3 forecasts from the operational UK Met Office limited area model. The total perturbation streamfunction, ψ'_{total}, is used to derive the interior QGPV on 50-mb levels ranging from 950mb to 150mb. Note that the period over which each cyclone has been considered depends on the relevant period of development.

(i) *Resulting characteristics of FASTEX cyclones*

An inspection of Figures 4-7 reveals that the most striking overall differences in forcing are between, on the one hand, the Type A and B cyclones (i.e. IOP9, 14 and 11A), and on the other hand, the Type C cyclone, IOP18. This latter cyclone had the deepest tropopause fold of any throughout the FASTEX period; hence, it might be expected that the upper-level PV distribution played a large role in the forcing of this cyclone. The time

* There are a number of differences, including the choice of level on which the vertical motion is calculated, between our approach and that of DBH. However, we are using the results of DBH as a guide to the type of cyclones studied, and these differences have little effect on the conclusions drawn here.

series shown in Figure 7 corresponds to a period of significant cyclonic deepening, during which a large upper-level PV anomaly appears to interact with the cyclone. As can be seen in Figure 7, one of the main individual contributions to the forcing is that of the upper-level PV self-generating term, $\omega(U,U)$. There are two interrelated reasons for this: (a) the upper-level PV anomaly is large enough in IOP18 to produce a significant $\nabla.\mathbf{Q}$ field via the interaction with the remaining part of the upper-level PV distribution which is attributable to the sloping tropopause; and (b) the upper-level anomaly in IOP18 is located relatively far down into the troposphere, so the associated $\nabla.\mathbf{Q}$ is large in the region close to the cyclone.

In the other cyclones, $\omega(U,U)$ is relatively small, attaining its largest values in the 'Type B', IOP11A. In the Type A and B cyclones, the upper-level PV distribution tends to be relatively "anomaly-free", dominated instead by the sloping tropopause (in contrast to point (a) mentioned just above). Hence, the vertical motion related to the upper-level PV in the Type A and B cyclones is mainly due the interaction of the 'sloping tropopause' streamfunction with the streamfunctions attributable to the more inhomogeneous low-level PV and/or surface temperature distribution. Moreover, these contributions are larger than any upper-level self-generated vertical motion which *does* exist, owing to the relative closeness of the low-level and boundary PV distributions to the cyclone.

The other important individual forcing term in IOP18 is $\omega(v_L,\theta_B)$. As was proposed in the previous section, this term should be large in *all* of the cyclones studied. It is worth stressing that this is the case even for a cyclone such as IOP18 where the upper-level PV anomaly is strikingly large. In other words, from a PV perspective, it appears that the low-levels are always important. Note that the terms $\omega(L,L)$, $\omega(U,L)$ and $\omega(U,B)$ are also important in IOP18. While each term on its own is (for most of the period) of secondary importance, their combined effect is nevertheless significant.

In the Type A cyclones (Figs. 4 and 5), the single most dominant component is $\omega(v_L,\theta_B)$. However, in a similar fashion to IOP18, $\omega(L,L)$, $\omega(U,L)$ and $\omega(U,B)$ all contribute significantly. Note that, while at first sight, $\omega(v_L,\theta_B)$ in IOP14 might appear to be the only term of importance, there is large cancellation between terms and both $\omega(L,L)$ and $\omega(U,B)$ also attain relatively large magnitudes. In the Type B cyclone, IOP11A (Fig. 6), it appears that the tropopause fold is strong enough so that the self-generating term $\omega(U,U)$ is slightly larger than in the Type A cyclones. However, this term is much smaller than in the case of IOP18, and the main involvement of the upper-level PV is still via the interaction terms. Note that in the Type B cyclone the upper-level PV plays a larger role early on and $\omega(v_L,\theta_B)$ becomes more significant at later stages. Such behaviour is less clear in the case of the Type A cyclones and it is tempting to speculate that the upper-level PV anomaly in the Type B cyclone in some sense causally precedes the lower-level PV.

From the PV perspective, the differences between the Type A and Type B cyclones appear to be more differences of degree than of kind. Whether or not we choose to view these relatively subtle differences as constituting different *classes* of cyclone from a 'PV thinking' viewpoint is a matter of debate which could be addressed by investigating many more cyclones. However, it is clear that the role played by the upper-level PV differs markedly between the Type C cyclone (during the period sampled) and the other cyclones. Hence, from a PV-attribution viewpoint of instantaneous cyclone forcing, there appear to be two main classes of cyclone: one where the effect of the upper-level PV is predominantly due to the interaction with the low-level PV and/or surface PV; and another where the self generating vertical motion of the upper-level PV plays a large role during part of the cyclone's lifetime.

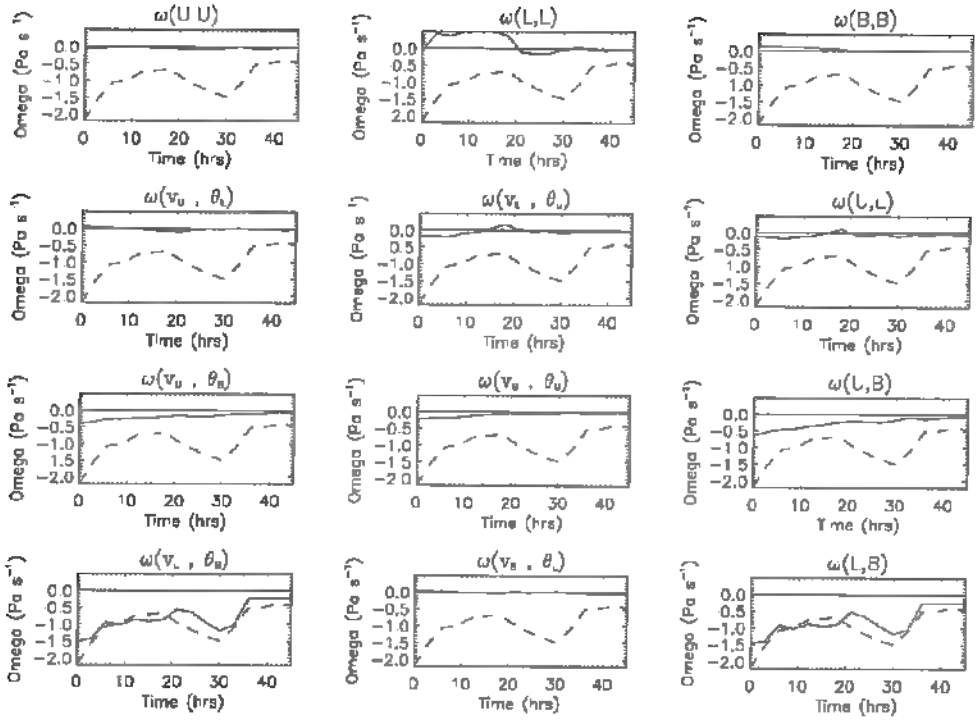

Figure 4. The time series of omega (dashed lines) and its constituent parts (full lines) at the position of maximum ascent in the case of the cyclone of IOP14. The top row of three plots are the self-generating terms. The remaining two rows of plots are the interaction terms. The first two plots in each row represent the potential temperature/ horizontal wind decomposition of omega, and the third plot in the row shows the sum of these two terms i.e. the decomposition in terms of streamfunction alone.

(d) *Indirect forcing and PV Surgery*

The methodology adopted here assesses the *direct* importance ("instantaneous" role) of a particular PV region on the development of a cyclone via the vertical motion it contributes to vortex-stretching near the cyclone. However, this method does not address to what extent one region of PV influences the development of either itself or another region of PV and/or the boundary component. Such *indirect* ("time-integrated") effects are important in that they lead to a complete causal description of the cyclone's evolution. For example, in the case of IOP18 we have shown that even though the upper-level PV contributes a large amount to the development of the cyclone, the $\omega(\mathbf{v}_L, \theta_B)$ is just as significant in the same 'direct' sense. However, this does not necessarily imply that the low-level PV is as important as the upper-level PV in determining the overall evolution of the cyclone. As the upper-level PV produces, by itself, a significant amount of vertical motion in the low-levels it is likely that it is responsible for a significant amount of the diabatic production of PV in that region. Furthermore, the advection of the low-level PV is probably dominated by the horizontal winds attributable to the upper-level PV. If it also transpires that the low-level PV has very little effect on the upper-level PV, then the cyclone might be said to be ultimately forced by the upper-level PV. By way of contrast in the case of IOP14, where the upper-level PV is less significant, it may be that low-level PV is responsible for its own development so that the cyclone is forced (both directly and indirectly) largely by the low-level PV and boundary components.

The distinction between direct and indirect forcing is related to the difference be-

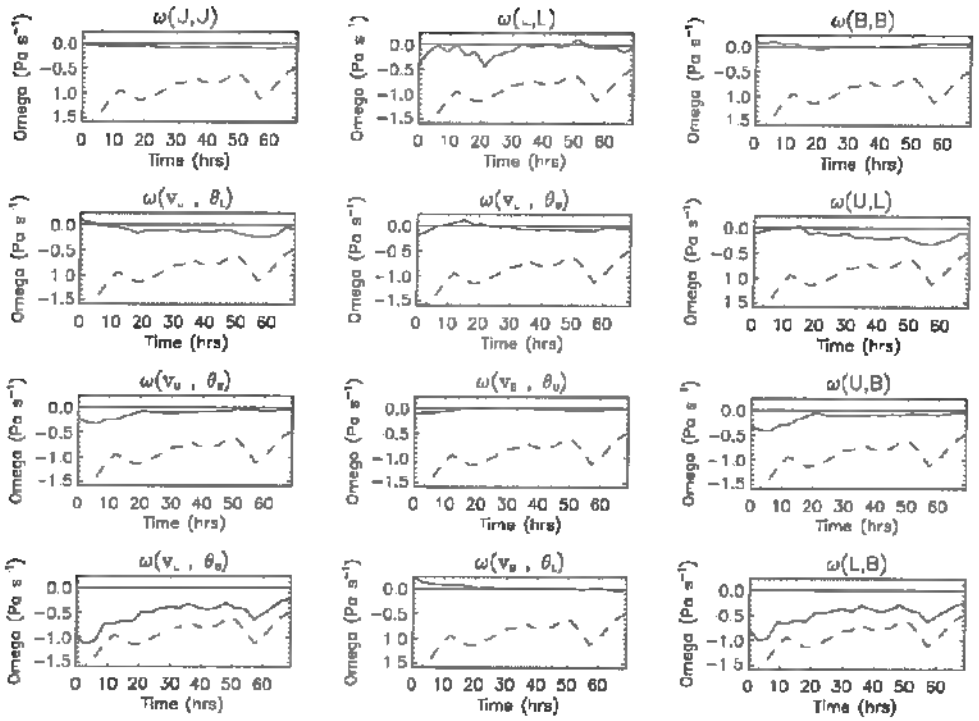

Figure 5. As in Figure 3, but for the case of IOP9

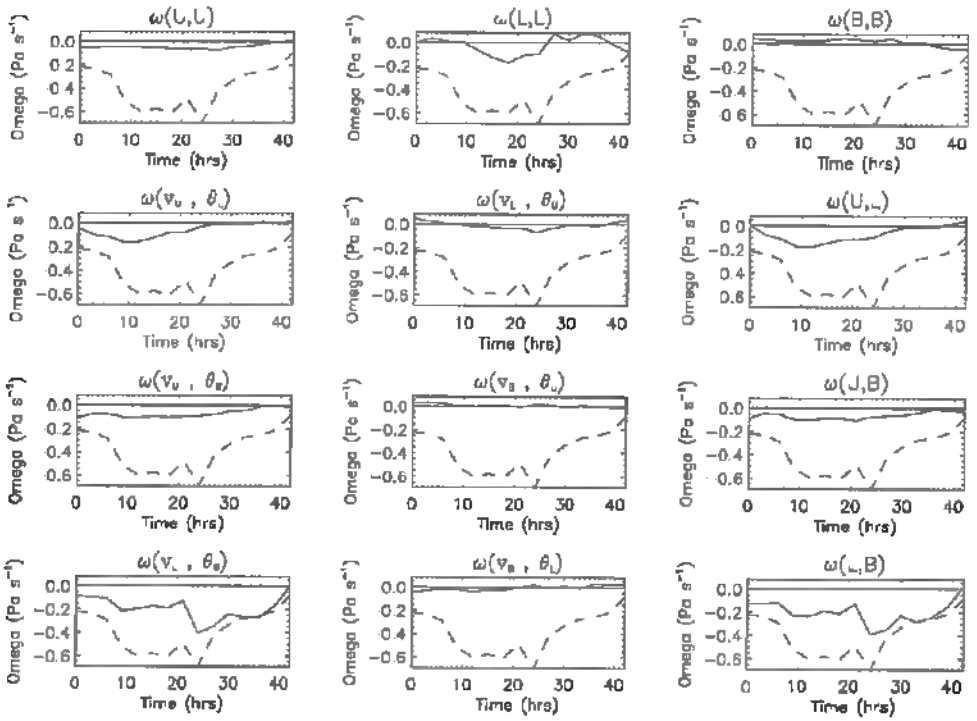

Figure 6. As in Figure 3 but for the case of IOP11A

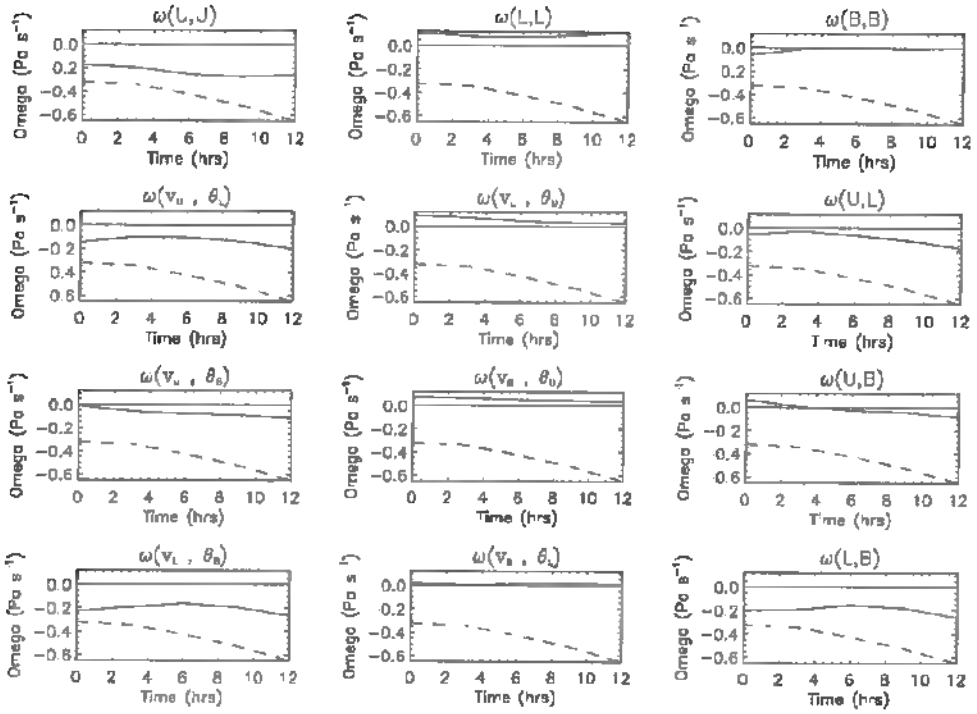

Figure 7. As in Figure 3 but for the case of IOP18

tween the form of instantaneous attribution described and adopted in this paper and the related methodology of so-called prognostic PV surgery. In the latter method, the impact on dynamical development attributable to a particular region of PV is assessed by taking the difference between a model run where the fields attributable to the region are removed and a control run where the fields are unaltered. Such a procedure directly yields information on the effect of the region on development. However it suffers from two drawbacks: (i) it fails to make the distinction between 'self-generating' and 'interaction' forcing; and (ii) the system is changed by the removal of PV, whereas the methodology presented here assesses the role of PV in the unaltered system. On the other hand, PV surgery avoids having to assess explicitly both the direct and indirect importance of PV and can easily incorporate the effects of diabatic processes. (To a certain extent, diabatic forcing can be viewed as being 'slaved' to the purely dynamical forcing. Hence, the results of the methodology presented here may be indicative of the importance of PV in the presence of diabatic processes.) Notwithstanding these differences, we might expect the two methodologies to yield similar results. According to the prognostic PV surgery described in Ahmadi-Givi & Craig (2001), the development of the Type C cyclone of IOP18 is dramatically diminished when the upper-level PV anomaly is removed and the upper-level PV anomaly fails to fully re-develop. On the other hand, their experiments where the low-level PV anomaly was removed led to less of an impact on development and the low-level PV was seen to re-develop. Furthermore, by considering the instantaneous fields attributable to each of the PV regions, they established that the evolution of the upper-level PV was essentially controlled by upper level dynamics. Hence, both PV-surgery and the methodology of the present study (when indirect forcing is taken into account) suggest that in the case of the Type C cyclone the upper-level PV dominates

the development of the cyclone.

5. Conclusions

The methodology presented in this paper enables the vertical motion attributable to a region of PV to be determined in an unambiguous manner, thereby providing a direct link between PV and dynamical development which was previously missing from QGPV-thinking. It has been shown how the total vertical motion may be decomposed into a number of 'self-generating' and 'interaction' terms. The self-generating terms correspond to the vertical motion that arises from one region of PV, whilst each interaction term results from the combined effect of two different regions of PV. The existence of the interaction terms, which makes the PV-attribution of vertical motion more complicated than the more traditional forms of vertical-motion attribution, is a consequence of the quadratic dependence of the vertical motion on streamfunction. It is possible to regard the interaction terms as arising from either the streamfunctions attributable to each of the two regions of PV, or from the horizontal velocity attributable to one PV region and the potential temperature attributable to the other region.

Vertical motion is a key quantity in diagnosing dynamical development and we have used the new methodology to assess the development of five FASTEX cyclones. We chose to partition the total PV distribution into three layers (upper, lower and lower boundary) for the purposes of simplicity and to facilitate comparison with the extended Petterssen-Smebye scheme of Deveson, Browning and Hewson. The method could, however, be applied using any other desired decomposition.

Each cyclone exhibited a number of common features, which we have been able to explain in terms of general principles. Of central importance in all of the cases studied, is the dominance of the term that arises from the interaction between the horizontal velocity attributable to the lower-level layer of PV and the potential temperature attributable to the boundary PV. This is due to the proximity of both PV regions to the cyclone location.

Deveson et al.(2002) classified cyclones into Types A, B and C. Types A and B correspond to the earlier classification of Petterssen and Smebye (1971) and Type C is an additional category strongly forced from upper levels. From a PV perspective, we found that there were only subtle differences between the Type A and B cyclones. For example, the upper-level PV layer played a more important role in the case of the Type B case. We have found that the most striking difference exhibited was between the Type A and B cyclones on the one hand, and the Type C cyclone on the other. A large enough upper level PV anomaly was present during part of the Type C cyclone's lifetime for the self-generating term associated with the upper-level PV to play a significant role in the forcing. In the Type A and B cyclones, however, the upper-level anomalies were not strong enough to have a major effect in themselves and the main influence of the upper-level PV was via interaction with the two lower PV regions.

It is worth stressing that, even in the case of the Type C cyclone, the low-level forcing term described above still played a very significant role. Hence, from the viewpoint of instantaneous forcing, the low-level PV is important even when there is a very strong upper-level PV anomaly present. However, in the case of the Type C cyclone, we have also argued, from the viewpoint of indirect forcing, that the upper-level PV is likely to be of greatest importance since it appears to generate and/or control low-level PV via its self-generating term.

The extent to which these case studies are representative of cyclones in general can only be gauged by applying the new methodology to a much larger sample of cyclones.

Such a procedure would be relatively straightforward to implement in an automated fashion.

Acknowledgement

We are grateful for the FASTEX-CSS EC Contract (ENV4-CT97-0625) which funded this work. We also thank Drs Paul Berrisford and Ross Bannister for useful discussions.

References

Bishop, C H and Thorpe, A. J. [illegible] Potential vorticity and the electrostatic analogy: *Quasi-geostrophic theory. Q. J. R. Meteorol. Soc.*, **120**, 713–731

Bretherton, F. P. 1966 Critical layer instability in baroclinic flows. *Q. J. R. Meteorol. Soc.*, **92**, 325–334

Clough, S. A., Davitt, C. S. A., and Thorpe, A. J. 1996 Attribution concepts applied to the omega equation. *Q. J. R. Meteorol. Soc.*, **122**, 1943–1962

Davies, H. C. and Bishop, C. H. 1994 Eady Edge Waves and Rapid Development. *J. Atmos. Sci.*, **51**, 1930–1946

Davis, A. C. and Emanuel, K. A. 1991 Potential Vorticity Diagnostics of Cyclogenesis. *Mon. Wea. Rev.*, **119**, 1929–1953

Deveson, A. C., Browning, K. A., and Hewson, T. D. 2002 A classification of FASTEX cyclones using a height-attributable quasi-geostrophic vertical-motion diagnostic. *Q. J. R. Meteorol. Soc.*, **128**, 93–117

Griffiths, M., Thorpe, A. J., and Browning, K. A. 2000 Convective destabilization by a tropopause fold diagnosed using potential- vorticity inversion *Q. J. R. Meteorol. Soc.*, **126**, 125–144

Hoskins, B. J., Draghici, I., and Davies, H. C. 1978 A new look at the w equation. *Q. J. R. Meteorol. Soc.*, **104**, 31–38

Hoskins, B. J., McIntyre, M. E, and Robertson, A. W. 1985 On the use and significance of isentropic potential vorticity maps. *Q. J. R. Meteorol. Soc.*, **111**, 877–946

Joly, A., Browning, K. A., Bessemoulin, P., Cammas, J. P., Caniaux, G., Chalon, J. P., Clough, S. A., Dirks, R., Emanuel, K. A., Eymard, L., Gall, R., Hewson, T., Hildebrand, P. H., Jorgensen, D., , Lalaurette, F., Langland, R. H., Lemaitre, Y., Mascart, P., Moore, J. A., Roux, P. O. G. P. F., Shapiro, M. A., Snyder, C., and Toth, Z. 1999 Overview of the field phase of the Fronts and Atlantic Storm-Track Experiment (FASTEX) project. *Q. J. R. Meteorol. Soc.*, **125**, 3131–3165

Mansfield, D. A. 1996 The use of potential vorticity as an operational forecast tool. *Meteorol. Appl.*, **3**, 195–210

Pettersen, S. and Smebye, S. J. 1971 On the development of extratropical cyclones. *Q. J. R. Meteorol. Soc.*, **97**, 457–482

Swarbrick, S. 2001 Applying the relationship between potential vorticity fields and water vapour imagery to adjust initial conditions in NWP *Meteorol. Appl.* , **8**, 221–228

Thorpe, A. J. 1997 Attribution and its application to mesoscale structure associated with tropopause folds. pp *Q. J. R. Meteorol. Soc.* , **123**, 2377–2400

CURRENT JCMM INTERNAL REPORTS

This series of JCMM Internal Reports, initiated in 1993, contains unpublished reports and also versions of articles submitted for publication. The complete set of Internal Reports is available from the National Meteorological Library on loan, if required.

1. **Research strategy and programme**
   K A Browning et al
   January 1993

2. **The GEWEX Cloud System Study (GCSS)**
   GEWEX Cloud System Science Team
   January 1993

3. **Evolution of a mesoscale upper tropospheric vorticity maximum and comma cloud from a cloud-free two dimensional potential vorticity anomaly**
   K A Browning
   January 1993

4. **The global energy and water cycle**
   K A Browning
   July 1993

5. **Structure of a midlatitude cyclone before occlusion**
   K A Browning and N Roberts
   July 1993

6. **Developments in systems and tools for weather forecasting**
   K A Browning and G Szejwach
   July 1993

7. **Diagnostic study of a narrow cold frontal rainband and severe winds associated with a stratospheric intrusion**
   K A Browning and R Reynolds
   August 1993

8. **Survey of perceived priority issues in the parametrizations of cloud-related processes in GCMs**
   K A Browning
   September 1993

9. **The effect of rain on longwave radiation**
   I Dharssi
   September 1993

10. **Cloud microphysical processes - a description of the parametrization used in the large eddy model**
    H Swann
    October 1993

11. **An appreciation of the meteorological research of Ernst Kleinschmidt**
    A J Thorpe
    May 1992

12. **Potential vorticity of flow along the Alps**
    A J Thorpe, H Volkert and Dietrich Heimann
    August 1992

13. **The representation of fronts**
    A J Thorpe
    January 1993

14. **A parametrization scheme for symmetric instability: test for an idealised flow**
C S Chan and A J Thorpe
February 1993

15. **The Fronts 92 Experiment: a Quicklook Atlas**
Edited by T D Hewson
November 1993

16. **Frontal wave stability during moist deformation frontogenesis**
Part 1: Linear wave dynamics
C H Bishop and A J Thorpe
May 1993

17 **Frontal wave stability during moist deformation frontogenesis**
Part 2. The suppression of non-linear wave development
C H Bishop and A J Thorpe
May 1993

18. **Gravity waves in sheared ducts**
S Monserrat and A J Thorpe
October 1993

19. **Potential vorticity and the electrostatics analogy: quasi-geostrophic theory**
C Bishop and A J Thorpe
November 1993

20. **Recent advances in the measurement of precipitation by radar**
A J Illingworth
April 1993

21. **Micro-physique et givrage: cloud microphysics and aircraft icing**
A J Illingworth
May 1993

22. **Differential phase measurements of precipitation**
M Blackman and A J Illingworth
May 1993

23. **Estimation of effective radius of cloud particles from the radar reflectivity**
N I Fox and A J Illingworth
May 1993

24. **A simple method of Dopplerising a pulsed magnetron radar**
A Hua, A J Illingworth and J Eastment
November 1993

25. **Radiation and polar lows**
George C Craig
February 1994

26. **Collected preprints submitted to the International Symposium on the Life Cycles of Extratropical Cyclones; Bergen, Norway, 27 June - 1 July 1994**
April 1994

27. **Convective frontogenesis**
Douglas J Parker and Alan J Thorpe
April 1994

28. **Improved measurement of the ice water content in cirrus using a total water evaporator**
Philip R A Brown and Peter N Francis
April 1994

29. **Mesoscale effects of a dry intrusion within a vigorous cyclone**
K A Browning and B W Golding
April 1994

30. **GEWEX Cloud System Study, Science Plan**
May 1994

31. **Parametrization of momentum transport by convectively generated gravity waves**
R Kershaw
May 1994

32. **Mesoscale Modelling Newsletter No 5**
May 1994

33. **Observations of the mesoscale sub-structure in the cold air of a developing frontal cyclone**
K A Browning, S A Clough, C S A Davitt, N M Roberts and T D Hewson
May 1994

34. **Longwave radiative forcing of a simulated tropical squall line**
Imtiaz Dharssi
July 1994

35. **On the nature of the convective circulation at a kata-cold front**
K A Browning
September 1994

36. **Collective preprints of papers submitted to the COST-75 International Seminar on Advanced Weather Radar Systems, Brussels, 20-23 September 1994**
November 1994

37. **Use of satellite imagery to diagnose events leading to frontal thunderstorms: Parts I and II of a case study**
K A Browning and N M Roberts
November 1994

38. **The role of spaceborne millimetre-wave radar in the global monitoring of ice cloud**
P R A Brown, A J Illingworth, A J Heymsfield, G M McFarquhar, K A Browning and M Gosset
December 1994

39. **Potential vorticity inversion**
Michal Ziemianski
October 1994

40. **Theory of mature tropical cyclones; a comparison between Kleinschmidt (1951) and Emanuel (1986)**
Suzanne L Gray
December 1994

41. **Dispersion and removal of pollutants during the passage of an atmospheric frontal system**
N R Gimson
December 1994

42. **The role of snow sublimation in frontogenesis**
D J Parker and A J Thorpe
December 1994

43. **Potential vorticity and the electrostatics Analogy: Ertel-Rossby formulation**
A J Thorpe and C H Bishop
December 1994

44. **Mesoscale aspect of extratropical cyclones: an observational perspective**
K A Browning
January 1995

45. **A polar low outbreak: evolution and mesoscale structures**
T D Hewson, G C Craig and C Claud
February 1995

46. **Generation of near-surface gusts of deep convection**
K Nakamura and R Kershaw
April 1995

47. **Attribution concepts applied to the Omega Equation**
S A Clough, C S A Davitt and A J Thorpe
June 1995

48. **Parametrization of mixed-phase cloud and precipitation**
Susan P Ballard and M Gerard Hutchinson
June 1995

49. **Short-range forecasting of stratocumulus: initialization prediction**
Susan P Ballard, Simon D Jackson and B Macpherson
June 1995

50. **Contributions of the JCMM/Dept of Meteorology Radar Group to the 27th AMS Radar Meteorology Conference, Vail October 1995**
June 1995

51. **Cold pools in shear**
Douglas J Parker
September 1995

52. **High-resolution analysis of frontal fracture**
K A Browning, S P Ballard and C S A Davitt
September 1995

53. **The albedo of broken cloud fields: calculations using a modified two stream radiation code**
Imtiaz Dharssi and Roy Kershaw
October 1995

54. **Parametrization of momentum transport by convection. I: theory and cloud modelling results**
R Kershaw and D Gregory
November 1995

55. **Variation of frontal structure along a cold front**
K A Browning and N M Roberts
November 1995

56. **Secondary frontal waves**
Douglas Parker
December 1995

57. **Objective fronts**
T D Hewson
March 1996

58. **Mesoscale analysis of the activation of a cold front during cyclogenesis**
K A Browning, N M Roberts and A J Illingworth
June 1996

59. **Investigation of different representations of rain in a 1-d evaporation model**
H Swann
May 1996

60. **Parametrization of diabatic processes in the inversion of the omega-equation**
M Athanassiadou and A J Thorpe
June 1996

61. **The role of the environmental flow in the development of secondary frontal cyclones**
I A Renfrew, A J Thorpe and A Joly
June 1996

62. **Consequences of the geostrophic momentum approximation on barotropic instability**
S Malardel, A J Thorpe and A Joly
June 1996

63. **Contributions to the AMS/RMS Conference on Mesoscale Processes**
Reading, 9-13 September 1996

64. **Vorticity and potential vorticity in stratified flows interacting with an isolated obstacle**
Jorge A Gutiérrez and A J Thorpe
September 1996

65. **Triple point development: two case studies**
Douglas Parker
September 1996

66. **Radar observations of wind-shear splitting within evolving atmospheric Kelvin-Helmholtz billows**
D Chapman and K A Browning
April 1997

67. **Cold frontal structure derived from radar wind profilers**
K A Browning, D Jerrett, J Nash, T Oakley and N M Roberts
May 1997

68. **The dry intrusion and its effect on the frontal, cloud and precipitation structure of extratropical cyclones**
K A Browning - Text of invited special lecture at the Spring Conference
of the Meteorological Society of Japan, University of Tsukuba, 22 May 1997

69. **Met. Office Unified Model data, diagnostics, graphics programs, and other observational data available from the JCMM through the aegis of the Universities Weather Research Network (UWERN).** (Plus supplement)
Peter Panagi and Ed Dicks
June 1997

70. **Contributions of the JCMM/Dept of Meteorology Radar Group to the 28th AMS Radar Meteorology Conference.** Austin, Texas
September 1997

71. **Sensitivity of short-range weather forecasts to local potential vorticity modifications**
Meral Demirtas and Alan Thorpe
July 1997

72. **Objective identification of frontal wave cyclones**
T D Hewson
August 1997

73. **Attribution and its application to mesoscale structure associated with tropopause folds**
A J Thorpe
September 1997

74. **The role of the environmental flow in the development of secondary frontal cyclones**
Ian A Renfrew, Alan J Thorpe and Craig H Bishop
September 1997

75. **Potential vorticity: a short history of its definitions and uses**
Alan J Thorpe and Hans Volkert
September 1997

76. **Superposing semi-geostrophic potential vorticity anomalies**
H R Birkett and A J Thorpe
September 1997

77. **Short period forecasting of catchment-scale precipitation.**
Part 1: the role of Numerical Weather Prediction
M A Pedder, M Haile and A J Thorpe
September 1997

78. **Verification of the tracking technique used in an experimental cloud motion wind inferring system**
Z Wang, K A Browning and G A Kelly
October 1997

79. **A preliminary study of Fourier series analysis for cloud tracking with GOES high temporal resolution images**
Z Wang
October 1997

80. **Analysis of an ex-tropical cyclone after reintensifying as a warm-core extratropical cyclone**
K A Browning, G Vaughan and P Panagi
November 1997

81. **A JCMM overview of FASTEX IOPs**
S A Clough, H W Lean, N M Roberts, H Birkett, J-P Chaboureau, R Dixon, M Griffiths, T D Hewson and A Montani
January 1998

82. **Programs for PV inversion and modification**
Meral Demirtas
December 1997

83. **Release of potential shearing instability in warm frontal zones**
D Chapman and K A Browning
February 1998

84. **The European Cloud-Resolving Modelling Programme (EUCREM)**
Summary Report from the coordinator
P W White
April 1998

85. **A frontal wave database**
T D Hewson
April 1998

86. **Layering observed in dropsoundings from IOP 1 of Fronts 92**
S A Clough
May 1998

87. **Use of wind-shear displays for Doppler radar data**
D Chapman and K A Browning
May 1998

88. **Radar estimates of rainfall rates at the ground in bright band and non-bright band events**
T J Smyth and A J Illingworth
June 1998

89. **Correction for attenuation of radar reflectivity using polarisation data**
T J Smyth and A J Illingworth
June 1998

90. **The effects of convection on chemical reactions and precipitation scavenging**
Neil R Gimson
July 1998

91. **How to use the display program DISP**
Nigel Roberts
August 1998

92. **Conceptual models of cyclogenesis**
Adrian T Semple
August 1998

93. **Observations of oblate hail using dual polarisation radar and implications for hail detection schemes**
T J Smyth, T M Blackman and A J Illingworth
September 1998

94. **The semigeostrophic diagnosis of vertical motion. Part I: Formulation and co-ordinate transformations**
Mike A Pedder and Alan J Thorpe
September 1998

95. **The semigeostrophic diagnosis of vertical motion. Part II: Results for an idealised baroclinic wave life cycle**
Alan J Thorpe and Mike A Pedder
September 1998

96. **Convective destabilisation by a tropopause fold diagnosed using potential vorticity inversion**
Morwenna Griffiths, Alan Thorpe and Keith Browning
October 1998

97. **Forecast skill of the ECMWF model using targeted observations during FASTEX**
A Montani, A J Thorpe, R Buizza and P Unden
October 1998

98. **Observations and model simulations of the FASTEX IOP 16 frontal wave - effects of sublimation**
Sid A Clough, Humphrey W Lean, Nigel M Roberts and Richard M Forbes
December 1998

99. **The application of conceptual models in NWP**
Adrian T Semple
January 1999

100. **Mesoscale analysis of arc rainbands in a dry slot**
K A Browning and N M Roberts
January 1999

101 **Interaction of mesoscale tropopause depressions with a warm-core cyclone: observational and model analyses, and sensitivity to analysis errors**
K A Browning, A J Thorpe, A Montani, D Parsons, M Griffiths, P Panagi and E M Dicks
February 1999

102. **The use of water vapour imagery and PV inversion to adjust initial conditions in NWP**
Sean J Swarbrick
February 1999
This report is no longer available; see Internal Report No.108

103. **Summary notes for a lecture course on Waves in the Atmosphere and Ocean**
A A White
March 1999

104. **Results of a questionnaire on the operational value of conceptual models (CMs) of fronts and cyclones**
N M Roberts & M V Young
July 1999

105. **Contributions to the Poster Session at the 1998 UWERN Annual Science Meeting**
assembled by A A White
August 1999

106. **The objective analysis of dropsonde data from FASTEX**
Richard Forbes, Sid Clough, Mark Dixon, Andy Macallan & Nigel Roberts
January 2000

107. *NWP Technical Report No.302*
Implications for Mesoscale Modelling from a Study of the FASTEX IOP 16 Mid-latitude Cyclone
Richard M Forbes, Humphrey W Lean, Nigel M Roberts and Peter A Clark
March 2000

108. *NWP Technical Report No.291*
The use of water vapour imagery and PV inversion to adjust initial conditions in NWP
Final Project Report
Sean J Swarbrick
September 1999

109. *NWP Technical Report No.294*
A guide to aspects of water vapour imagery interpretation: the significance of dry regions
Nigel M Roberts
January 2000

110. *NWP Technical Report No.300*
The relationship between water vapour imagery and thunderstorms
Nigel M Roberts
February 2000

111. *NWP Technical Report No.293*
Holomorphic structures in hydrodynamical models of nearly geostrophic flow
V N Roubtsov and I Roulstone
January 2000

112. *NWP Technical Report No.301*
Multi-sensor synthesis of the mesoscale structure of a cold-air comma cloud system
K A Browning, P Panagi and E M Dicks
March 2000

113. *NWP Technical Report No.307*
Observations of stratospheric air entering the circulation of a polar low
K A Browning and E M Dicks
May 2000

114. *NWP Technical Report No.309*
Wind profiler – Unified Model comparison statistics
Peter Panagi & Ed Dicks
March 2000

115. *NWP Technical Report No.310*
Towards a similarity theory of moist convective updrafts
Olaf Stiller and George C Craig
May 2000

116. *NWP Technical Report No.312*
The mystery of striated cloud heads in satellite imagery
R S Dixon, K A Browning and G J Shutts
April 2000

117. *NWP Technical Report No.313*
MDIAG: a Fortran 90 program to compute diagnostics on pressure levels from Unified Model data on model levels
Peter Panagi
June 2000

118. *NWP Scientific Paper No.56*
Rearrangements of functions with applications to meteorology and ideal fluid flow
R J Douglas
June 2000

119. *NWP Technical Report No.320*
Tests of New Dynamics Model on the FASTEX IOP16 case
Humphrey Lean
September 2000

120. *NWP Scientific Paper 57*
A classification of FASTEX cyclones using a height-attributable QG vertical motion diagnostic
A C L Deveson, K A Browning, T D Hewson
September 2000

121. *NWP Scientific Paper 59*
Measurements of dissipation rate in frontal zones
D.Chapman, K A Browning
August 2000

122. *NWP Technical Report 331*
Not Issued

123. *NWP Technical Report 337*
A Case Study of High Resolution Fog Forecasts with the New Dynamics
P. Clark
November 2000

124. *NWP Technical Report 338*
Comparison of ECMWF Winter-Season Cloud Fraction with Radar Derived Values
Robin J. Hogan, Christian Jakob, Anthony J. Illingworth
January 2001

125. *NWP Technical Report 339*
Deriving Cloud overlap statistics from radar
Robin J. Hogan, Anthony J. Illingworth
January 2001

126. *NWP Technical Report 344*
Results from simulations of an organised convective event using the New Dynamics at 12, 4 and 2km resolution.
Nigel Roberts
January 2001

127 *NWP Technical Report 348*
A North Atlantic Survey of Cyclogenesis in 1999: Unified Model Performance in Short Range Forecasts & The Relationship Between Potential Vorticity, Water Vapour Imagery and Analysis Accuracy.
Adrian Semple
March 2001

128 NWP Scientific Paper 61
Are there higher-accuracy analogues of semigeostrophic theory?
Ian Roulstone, Michael E. McIntyre
June 2001

129 NWP Scientific Paper 62
Stacked slantwise convective circulations
K A Browning, D Chapman, R S Dixon
April 2001

130 NWP Technical Report 357
A Meteorological Assessment of the Geostrophic Co-ordinate Transform and Error Breeding System when used in 3D Variational Data Assimilation.
Adrian Semple
June 2001

131 NWP Scientific Paper 63
The dynamics of a mid-latitude cyclone with very strong latent heat release
Farhang Ahmadi-Givi, George Craig
July 2001

132 NWP Scientific Paper 64
A Study of the Effects of Horizontal and Vertical Resolution in the New Dynamics representation of FASTEX IOP16
Humphrey Lean
October 2001

133 NWP Scientific Paper 66
Modelling Low Level Winds with the Met Office New Dynamics Model
Rachel Anne Capon
9 May 2002

134 NWP Scientific Paper 67
Layer-wise attribution of vertical motion and the influence of potential-vorticity anomalies on synoptic development
M Dixon, A. J. Thorpe, K. A. Browning
May 2002

Met Office Joint Centre for Mesoscale Meteorology Department of Meteorology
University of Reading PO Box 243 Reading RG6 6BB United Kingdom
Tel: +44 (0)118 931 8425 Fax: +44 (0)118 931 8791
www.metoffice.com